

Scanning Tunneling Microscopy

Ada Della Pia and Giovanni Costantini
Department of Chemistry, The University of
Warwick, Coventry, UK

Definition

A scanning tunneling microscope (STM) is a device for imaging surfaces with atomic resolution. In STM, a sharp metallic tip is scanned over a conductive sample at distances of a few Å while applying a voltage between them. The resulting tunneling current depends exponentially on the tip-sample separation and can be used for generating two-dimensional maps of the surface topography. The tunneling current also depends on the sample electronic density of states, thereby allowing to analyze the electronic properties of surfaces with sub-nm lateral resolution.

Overview and Definitions

If two electrodes are held a few Å apart and a bias voltage is applied between them, a current flows even though they are not in contact, due to the quantum mechanical process of electron tunneling. This current depends exponentially on the electrode separation, and even minute, subatomic variations produce measurable current changes. In 1981, Gerd Binnig and Heinrich Rohrer at IBM in Zürich realized that this phenomenon can be used to build a microscope with ultrahigh spatial resolution [1], if one of the electrodes is shaped as a sharp tip and is scanned across the surface of the other (Fig. 1). Moreover, since the tunneling current depends also on the electronic properties of the electrodes, this microscope has the ability to probe the electronic density of states of surfaces at the atomic scale. A few years later, Don Eigler at IBM in Almaden, showed that, due to the extremely localized interaction between tip and sample, it is also possible to use this instrument to manipulate individual atoms, to position them at arbitrary locations and therefore to build

artificial structures atom-by-atom [2]. This remarkable achievement brought to reality the visionary predictions made by Richard Feynman in his famous 1959 lecture “*There’s plenty of room at the bottom*” [3].

The construction of this instrument, dubbed the scanning tunneling microscope (STM), was awarded the 1986 Nobel Prize in Physics and has since then revolutionized contemporary science and technology. The STM has enabled individual atoms and molecules to be imaged, probed, and handled with an unprecedented precision, thereby essentially contributing to our current understanding of the world at the nanoscale. Together with its offspring, the atomic force microscope (AFM) [► AFM], the STM is considered as the main innovation behind the birth of nanotechnology.

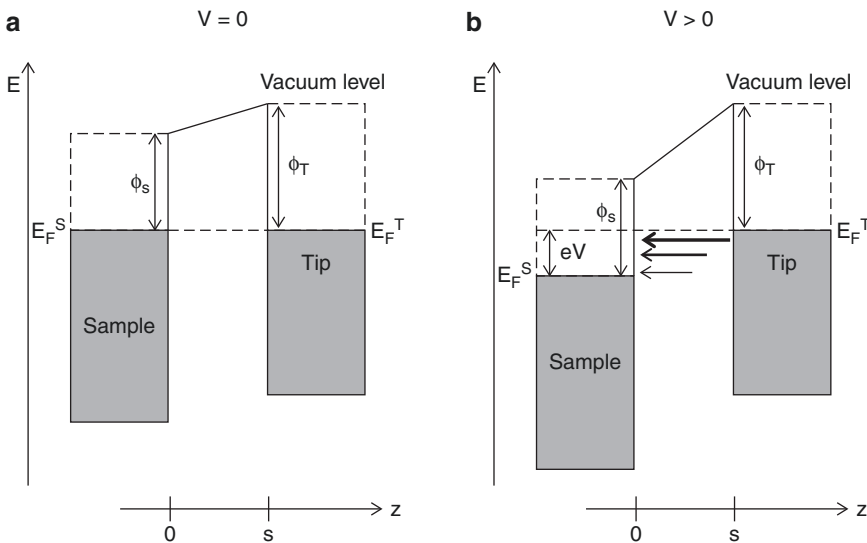
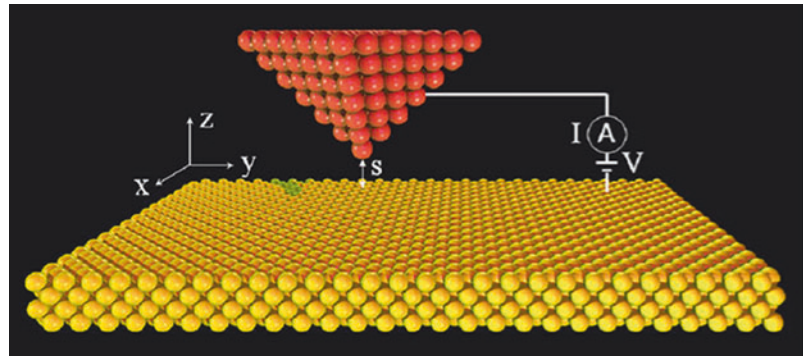
This entry will start with a discussion of the physical principles and processes at the heart of STM in section “[Theory of Tunneling](#).” This will be followed by a description of the experimental setup and the technical requirements needed for actually operating such a microscope in section “[Experimental Setup](#).” Section “[STM Imaging](#)” is dedicated to the most frequent use of STM, namely imaging of surfaces, while section “[Scanning Tunneling Spectroscopy](#)” gives a brief account of the spectroscopic capabilities of this instrument. Finally, section “[Applications](#)” discusses several applications and possible uses of STM.

Theory of Tunneling

Figure 2 is a schematic representation of the energy landscape experienced by an electron when moving along the z axis of a metallic-substrate/insulator/metallic-tip tunneling junction. The following treatment can easily be extended to include also semiconducting tips or samples. Usually, the tip and the sample are not made of the same material and therefore have different work functions, ϕ_T and ϕ_S , respectively. At equilibrium, the two metals have a common Fermi level, resulting in an electric field being established across the gap region and in different local vacuum levels,

Scanning Tunneling Microscopy,

Fig. 1 Schematic representation of a STM. Tip and sample are held at a distance s of a few Å and a bias voltage V is applied between them. The resulting tunneling current I is recorded while the tip is moved across the surface. The coordinate system is also shown



Scanning Tunneling Microscopy, Fig. 2 Energy potential perpendicular to the surface plane for an electron in a tip-vacuum-sample junction. z is the surface normal direction, and s is the tip-sample distance. The gray boxes represent the Fermi-Dirac distribution at 0 K. $\phi_{T,S}$ and $E_F^{T,S}$ are the work functions and the Fermi levels of tip and sample, respectively. (a) Tip and sample in electrical

equilibrium: a trapezoidal potential barrier is created. (b) Positive sample voltage V : the electrons tunnel from occupied states of the tip into unoccupied states of the sample. The thickness and length of the arrows indicate the exponentially decreasing probability that an electron with the corresponding energy tunnels through the barrier

depending on the difference $\phi_T - \phi_S$ (Fig. 2a). Since the work functions in metals are of the order of several eV, the potential in the gap region is typically much higher than the thermal energy kT and thus acts as a barrier for sample and tip electrons. A classical particle cannot penetrate into any region where the potential energy is greater than its total energy because this requires a negative kinetic energy. However, this is possible for electrons which, being quantum mechanical objects, are described by delocalized wave functions. This

phenomenon goes under the name of *quantum tunneling*. In an unpolarized tip-sample junction the electrons can tunnel from the tip to the sample and vice versa, but there is no net tunneling current. On the contrary, if a voltage V is applied between sample and tip, the Fermi level of the former is shifted by $-eV$ and a net tunneling current occurs, whose direction depends on the sign of V (Fig. 2b). Here the convention is adopted to take the tip as a reference since experimentally the voltage is often applied to the sample while the tip is grounded. If

V is the bias voltage, the energy for an electron in the sample will change by $-eV$, that is, it will decrease for positive values of V .

The tunneling current can be evaluated by following the time-dependent perturbation approach developed by Bardeen [4, 5]. The basic idea is to consider the isolated sample and tip as the unperturbed system described by the stationary Schrödinger equations:

$$(\mathcal{T} + \mathcal{U}_s)\psi_\mu = E_\mu\psi_\mu \quad (1)$$

and

$$(\mathcal{T} + \mathcal{U}_T)\chi_\nu = E_\nu\chi_\nu \quad (2)$$

where \mathcal{T} is the electron kinetic energy. The electron potentials \mathcal{U}_s and \mathcal{U}_T and the unperturbed wavefunctions ψ_μ and χ_ν are nonzero only in the sample and in the tip, respectively. Based on this, it can be shown [5] that the transition probability per unit time $w_{\mu\nu}$ of an electron from the sample state ψ_μ to the tip state χ_ν is given by Fermi's golden rule:

$$w_{\mu\nu} = \frac{2\pi}{\hbar} |M_{\mu\nu}|^2 \delta(E_\nu - E_\mu) \quad (3)$$

where the matrix element is:

$$M_{\mu\nu} = \int \chi_\nu^*(\vec{x}) \mathcal{U}_T(\vec{x}) \psi_\mu(\vec{x}) d^3 \vec{x}. \quad (4)$$

The δ function in Eq. 3 implies that the electrons can tunnel only between levels with equal energy, that is, (Eq. 3) accounts only for an *elastic tunneling* process. The case of an inelastic tunneling process will be considered in section “**Scanning Tunneling Spectroscopy**.” The total current is obtained by summing $w_{\mu\nu}$ over all the possible tip and sample states and by multiplying this by the electron charge e . The sum over the states can be changed into an energy integral by considering the density of states (DOS) $\rho(E) : \sum \rightarrow 2 \int f(\varepsilon) \rho(\varepsilon) d\varepsilon$, where the factor 2 accounts for the spin degeneracy while f , the Fermi–Dirac distribution function, takes

into consideration Pauli's exclusion principle and the electronic state population at finite temperatures.

As a consequence, the total current can be written as:

$$I = \frac{4\pi e}{\hbar} \int_{-\infty}^{\infty} [f_T(E_F^T - eV + \varepsilon) - f_S(E_F^S + \varepsilon)] \times \rho_T(E_F^T - eV + \varepsilon) \rho_S(E_F^S + \varepsilon) |M|^2 d\varepsilon \quad (5)$$

where EF is the Fermi energy and the indexes T and S refer to the tip and the sample, respectively. Equation 5 already accounts for the movement of electrons from the sample to the tip and vice versa.

Several approximations can be made to simplify Eq. 5 and to obtain a manageable analytical expression for I . If the thermal energy $k_B T \ll eV$, the Fermi–Dirac distributions can be approximated by step functions and the total current reduces to:

$$I = \frac{4\pi e}{\hbar} \int_0^{eV} \rho_T(E_F^T - eV + \varepsilon) \rho_S(E_F^S + \varepsilon) |M|^2 d\varepsilon \quad (6)$$

(Note that Eq. 6 is valid only for $V > 0$. For $V < 0$ the integrand remains identical but the integration limits become $-e|V|$ and 0). In this case, only electrons with an energy differing from E_F by less than eV can participate to the tunneling current. This can be directly seen in Fig. 2b for the case of positive sample bias: tip electrons whose energy is lower than $E_F^T - eV$ cannot move because of Pauli's exclusion principle, while there are no electrons at energies higher than E_F^T . The main problem in determining expression (Eq. 5) is, however, the calculation of the tunneling matrix elements M since this requires a knowledge of the sample and the tip wave functions, which can be very complicated. On the other hand, for relatively small bias voltages (in the ± 2 V range), Lang [6] showed that a satisfactory approximation of $|M|^2$ is given by a simple one-dimensional WKB tunneling probability. In the WKB approximation [7], the probability $D(\varepsilon)$

that an electron with energy ε tunnels through a potential barrier $U(z)$ of arbitrary shape is expressed as:

$$D(\varepsilon) = \exp\left\{-\frac{2}{\hbar} \int_0^s [2m(U(z) - \varepsilon)]^{\frac{1}{2}} dz\right\}. \quad (7)$$

This semiclassical approximation is applicable if ($\varepsilon \ll U$) which is generally satisfied in the case of metal samples where the work function is of the order of several eV. In order to obtain a simple analytical expression for D , the trapezoidal potential barrier of a biased tip-sample junction (see Fig. 2b) is further approximated with a square barrier of average height $\phi_{\text{eff}}(V) = (\phi_T + \phi_S + eV)/2$. By using this, the integral in Eq. 7 becomes:

$$D(\varepsilon, V, s) = \exp(-2ks) \quad (8)$$

where

$$k = \sqrt{\frac{2m}{\hbar^2} (\phi_{\text{eff}} - \varepsilon)}. \quad (9)$$

In order to evaluate k , it must be noted that electrons closest to the Fermi level experience the lowest potential barrier and are therefore characterized by an exponentially larger tunneling probability (see Fig. 2b). Thus, in a first approximation, it can be assumed that only these electrons contribute to the tunneling current which, for positive bias, is equivalent to set $\varepsilon \approx eV$ in Eq. 9. Moreover, if the bias is much smaller than the work functions, eV can be neglected, resulting in

$$k \cong \frac{\sqrt{m(\phi_T + \phi_S)}}{\hbar} = 5.1 \sqrt{\frac{\phi_T + \phi_S}{2}} \text{ nm}^{-1} \quad (10)$$

where the work functions are expressed in eV. Using typical numbers for metallic work functions, the numerical value of the inverse decay length $2k$ in Eq. 8 becomes of the order of 20 nm^{-1} . Therefore, variations in s of 1 \AA correspond to one order of magnitude changes in the tunneling probability and, as a consequence, in the measured current. This very high sensitivity

provides the STM with a vertical resolution in the picometer regime. The lateral resolution of STM depends on how different points of the tip contribute to the total tunneling current. By considering a spherical tip shape with radius R , most of the current originates from the central position since this is closest to the surface. A point laterally displaced by Δx from the tip center is $\Delta z \approx \frac{\Delta x^2}{2R}$ further away from the substrate (higher order Δx terms are neglected in this evaluation). As a consequence, with respect to the tip center, the corresponding tunneling probability is reduced by a factor:

$$\exp\left(-2k \frac{\Delta x^2}{2R}\right). \quad (11)$$

By considering a tip radius $R \approx 1 \text{ nm}$, the current changes by one order of magnitude for variations $\Delta x = 3 \text{ \AA}$. The actual lateral resolution is typically smaller than this upper limit and can reach down to fractions of an \AA . Its specific value however depends on the precise shape of the tip which is unknown a priori. These values, together with the vertical resolution discussed above, lie at the basis of the STM atomic imaging capabilities.

Finally, if the tunneling probability (Eq. 8) is substituted for the tunneling matrix $|M|^2$ in Eq. 6, the total tunneling current can be expressed as:

$$I = \frac{4\pi e}{\hbar} \int_0^{eV} \rho_T(E_F^T - eV + \varepsilon) \rho_S(E_F^S + \varepsilon) e^{-2ks} d\varepsilon. \quad (12)$$

Therefore, for a fixed lateral position of the tip above the sample, the tunneling current I depends on the tip-sample distance s , the applied voltage V and the tip and sample density of states ρ_T and ρ_S , respectively.

Experimental Setup

As seen in the previous section, variations of 1 \AA in s induce changes in the tunneling probability of one order of magnitude. The exponential dependence in Eq. 8 is responsible for the ultimate spatial resolution of STM but places stringent

constraints on the precision by which s must be controlled, as well as on the suppression of vibrational noise and thermal drift. Moreover, typical tunneling currents are in the 0.01–10 nA range, requiring high gain and low noise electronic components. The following subsections are dedicated to a general overview of technologies and methods used to meet these specifications.

Scanner and Coarse Positioner

The extremely fine movements of the tip relative to the sample required for operating an STM are realized by using piezoelectric (► [Piezoresistivity](#)) ceramic actuators (*scanners*) which expand or retract depending on the voltage difference applied to their ends. In a first approximation, the voltage-expansion relation can be considered as linear with a proportionality factor (piezo constant) usually of few nanometer/Volt. The main requirements for a good scanner are: high mechanical resonance frequencies, so as to minimize noise vibrations in the frequency region where the feedback electronics operates (see section “[Electronics and Control System](#)”); high scan speeds; high spatial resolution; decoupling between x , y , and z motions; minimal hysteresis and creep; and low thermal drift. Although several types of STM scanner have been developed, including the bar or tube tripod, the unimorph disk and the bimorph [8], the most frequently used is a single piezoelectric tube whose outer surface is divided into four electrode sections of equal area. By applying opposite voltages between the inner electrode and opposite sections of the outer electrode, the tube bends and a lateral displacement is obtained. The z motion is realized by polarizing with the same voltage the inner electrode in respect to all four outer electrodes. By applying several hundred Volts to the scanner, lateral scan widths up to 10 μm and vertical ones up to 1 μm can be obtained, while retaining typical lateral and vertical resolutions of 0.1 and 0.01 nm, respectively.

While scanning is typically done by one individual piezoelectric element, larger displacements up to several millimeters are needed to bring the tip in close proximity to the sample, to move it to different regions of the surface or to exchange

samples or tips. These are achieved by mounting the scanner onto a coarse position device. Several designs have been developed to this aim including micrometric screws driven either manually or by a stepper motor, piezoelectric walkers like the louse used in the first STM [9] or the inch-worm [10], magnetic walkers where the movement is obtained by applying voltage pulses to a coil with a permanent magnet inside and piezoelectric driven stick-slip motors, as the Besocke-beetle [11] or the Pan motor [12].

Electronics and Control System

The voltages driving the piezoelectric actuators and their temporal succession and duration are generated by an electronic control system. The electronics are also used to bias the tunneling junction, to record the tunneling current and to generate the STM images. In most of the modern instruments, these tasks are digitally implemented by a computer interfaced with digital to analog (DAC) and analog to digital (ADC) converters. The tunneling current is amplified by a high gain I–V converter (10^8 – 10^{10} V/A) usually positioned in close proximity of the tip, so as to reduce possible sources of electronic interference. This signal is then acquired by an ADC and processed by the control system. DACs are used to apply the bias voltage (from a few mV to a few V) between tip and sample and, in conjunction with high voltage amplifiers, to polarize the piezo elements. A feedback loop is integrated into the control system and is activated during the frequently used *constant current* imaging mode (see section “[STM Imaging](#)”). By acting on the z motion of the scanner, the feedback varies s to keep the tunneling current constant. This is controlled by a proportional-integral and derivative (PID) filter whose parameters can be set by the operator. Finally, a lock-in amplifier is often used to improve the signal-to-noise ratio in scanning tunneling spectroscopy (STS) measurements (see section “[Scanning Tunneling Spectroscopy](#)”).

Tip

Sharp metal tips with a low aspect ratio are essential to optimize the resolution of the STM images and to minimize flexural vibrations of the tip,

respectively. Ideally, in order to obtain atomically resolved topographies and accurate spectroscopic measurements, the tip should be terminated by a single atom. In this case, because of the strong dependence on the tip-sample separation (see section “[Theory of Tunneling](#)”), most of the tunneling current would originate from this last atom, whose position and local DOS would precisely determine the tunneling conditions. In practice, however, it is almost impossible to determine the exact atomic configuration of the tip and the actual current is often due to a number of different atoms. This is still compatible with good tunneling conditions as long as these atoms are sufficiently localized (in order to avoid “multiple tip effects”) and their structural and chemical state remains constant during scanning.

The most commonly used methods to produce STM tips are to manually cut or to electrochemically etch thin wires of platinum-iridium and tungsten, respectively. These materials are chosen because of their hardness, in order to prevent tips becoming irreversibly damaged after an accidental crash. Other metallic elements and even semiconductor materials have been used as tips for specific STM applications. Due to their chemical inertness, Pt-Ir tips are often used to scan in air on atomically flat surfaces without the need of any further processing. However, they typically have inconsistent radii, while etched W tips are characterized by a more reproducible shape. These latter have the drawback that a surface oxide up to 20 nm thick is formed during etching or exposure to air. For this reason, W tips are mostly used in ultrahigh vacuum (UHV) where the oxide layer can be removed through ion sputtering and annealing cycles. Prior to use, tips are often checked by optical microscopy, scanning electron microscopy (► [SEM](#)), and field ion microscopy or transmission electron microscopy (► [TEM](#)). The quality of a tip can be further improved during scanning by using “*tip forming*” procedures, including pulsing and controlled crashing into metal surfaces. These processes work because the desorption of adsorbed molecules or the coating with atoms of the metallic substrate can produce a more stable tip apex. If STM is performed in polar liquids (► [EC-STM](#)), electrochemical processes might generate Faradaic

or non-Faradaic currents which can be of the same order of magnitude or even larger than the tunneling current. In order to minimize these effects, the tip, except for its very apex, must be coated with an insulating material.

Vibration Isolation

A low level of mechanical noise is an essential requirement for any type of scanning probe microscopy. For this reason, the core of a STM, where the tip-sample junction is located, is always equipped with one or several types of vibration damping systems. These can be stacks of metal plates separated by elastic spacers, suspension springs, or eddy current dampers composed of copper elements and permanent magnets. The low-frequency components of mechanical noise (<10 Hz), which are the most difficult to eliminate, are minimized by building a small and rigid STM with a high resonance frequency. Depending on the overall size and weight of the microscope, further noise damping strategies can be adopted. Smaller, typically ambient conditions STMs can be placed on metal or granite slabs suspended by springs or bungee cords or floating on pneumatic isolators. Sometimes, piezo-driven, feedback-controlled active vibration suppressors are also combined with passive systems. Larger versions of pneumatic isolators and active damping are often used to float the frames and the chambers of big UHV STMs. The laboratory where a STM instrument is located also plays an essential role for its performance. Ground floor rooms are always preferred since they minimize low-frequency natural building oscillations, which can be very difficult to counteract. High-resolution instruments are sometimes placed on large concrete blocks which are separated from the rest of the laboratory floor and rest either on a sand bed, an elastomer barrier or on second-stage pneumatic isolators. Moreover, they are also often surrounded by an acoustically insulating box. All these systems essentially act as low-pass mechanical filters whose effectiveness improves with decreasing cutoff frequencies, that is, with increasing mass and decreasing rigidity. For this reason, the body of a STM is typically a relatively heavy block of metal and the frames, slabs, and

vacuum chambers supporting or containing the microscope often have a considerable weight.

Setups for Different Environments and Temperatures

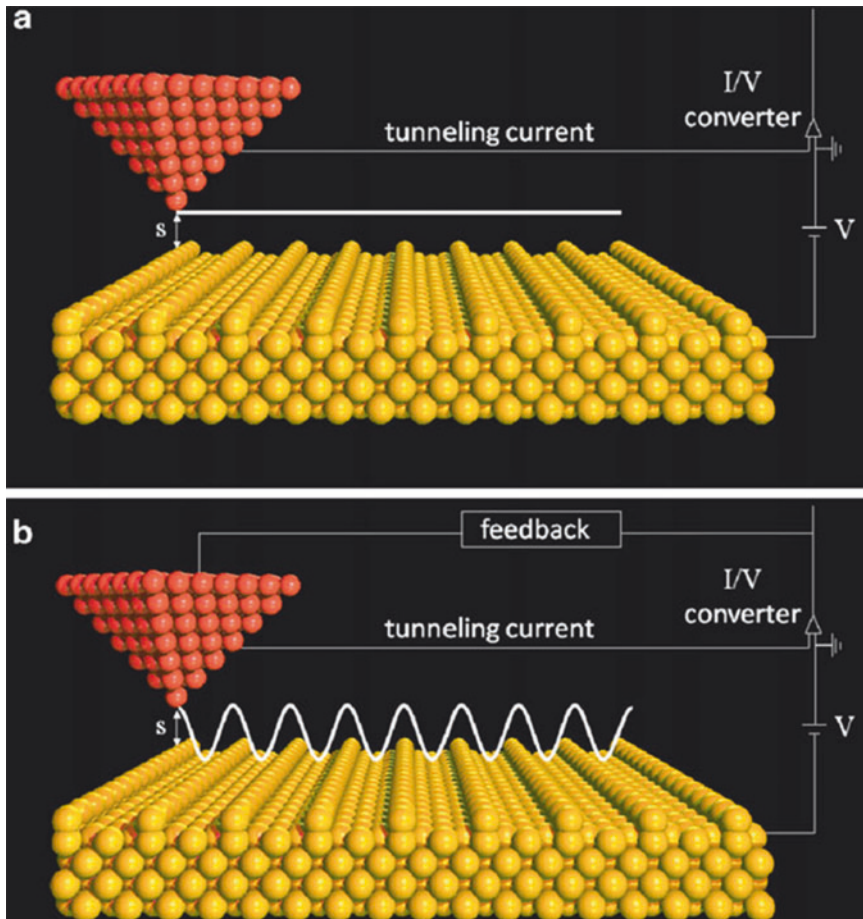
Different types of STMs have been developed that can operate in various environments such as air, inert atmosphere (N_2 , Ar), vacuum, high pressure, liquid, or in an electrochemical cell. The core of the different instruments is essentially the same, although the experimental chambers and setups in which they are located can vary substantially. Ambient condition STMs are typically quite compact and rigid and do not need elaborated anti-vibrational mechanisms. On the other hand, since sound waves represent a major problem, atmospheric pressure STMs are usually contained in an acoustic enclosure. A STM operating in vacuum must be hosted in a chamber with vibration-free pumps (typically ionic pumps for UHV) and must be equipped with sophisticated sample and tip manipulation mechanisms. Such systems often also have an in situ surface preparation stage allowing the handling of samples without air exposure.

STM can be performed at high pressures (1–30 bar) by installing the microscope head into gas manifolds under conditions similar to those used in industrial catalytic processes. Also in this case, sample and tip manipulation and preparation stages are mandatory parts of the system. Since these types of studies are typically performed at elevated temperatures (up to 600 K) and in the presence of highly reactive gases, the metallic parts of the STM scanner and of the chamber are often gold plated, the volume of the STM chamber is kept as small as possible and the tip material is chosen to be inert toward the gases [13]. Moreover, low voltages are used for polarizing the piezos in order to avoid gas discharges at intermediate pressures (10^{-3} –10 mbar) and shields are added to protect the STM from the deposition of conductive materials which could create electrical shorts.

STM at the liquid/solid interface and electrochemical STM (EC-STM) (► [EC-STM](#)) need the tip and sample to be inside a liquid cell which, in turn, may be placed in a humidity-controlled atmosphere. In the case of low vapor pressure liquids, the STM can be simply operated under

ambient conditions by dipping the tip into a liquid droplet deposited on the sample. A special coating must be applied to the tip when working with polar liquids (see section “[Tip](#)”).

STM can also be performed at different temperatures (in vacuum or controlled atmosphere chambers): variable temperature STM (VT-STM) able to cover the 5–700 K range, low temperature STM (LT-STM) operating at 77 K or 5 K and even milli-Kelvin STM instruments are currently available. A VT-STM is typically used to study thermally activated processes such as diffusion and growth, phase transitions, etc. These systems have sample heating and cooling stages which can be operated in a combined way so as to achieve a very precise temperature stabilization. Resistive heating is normally employed to increase the temperature, while both flow and bath cryostats with liquid nitrogen or helium as cryogenic fluids are used to reduce it. Continuous flow cryostats offer a high flexibility in temperature but are characterized by lower thermal stability, by inherent mechanical vibrations and do not easily attain temperatures below 20 K. Bath cryostats are more stable, are able to reach lower temperatures but are often also much bulkier (e.g., in order to limit the He consumption rate, a liquid He cryostat is actually a double-stage cryostat with an outer liquid nitrogen mantle). For most of these instruments the variable temperature capabilities refer to the possibility of choosing different (fixed) temperatures at which the microscope is run. However, few systems endowed with specific position tracking and drift compensating capabilities allow a “true” variable temperature operation where the same surface area can be imaged with atomic resolution while its temperature is changed. LT-STMs are operated at a fixed temperature and are typically inserted inside double stage cryostats which significantly complicates the tip and sample access. However, these instruments are extremely stable with a very low thermal drift and are therefore the best choice for STS and manipulation experiments (see sections “[Scanning Tunneling Spectroscopy](#)” and “[Applications](#)”). Milli-Kelvin STMs enable temperatures to be reached where extremely interesting magnetic, quantum Hall physics and superconductivity phenomena occur. Moreover, the thermal broadening of electronic



Scanning Tunneling Microscopy, Fig. 3 Schematic representation of (a) the constant height and (b) the constant current imaging modes, respectively. The *thick lines* represent the trajectory followed by the tip

features is strongly reduced, which is required for high-resolution measurements. These systems operate based on the evaporative cooling of liquid ^3He to temperatures of about 300 mK or liquid ^3He and ^4He mixtures below 10 mK. The STM heads can be further placed inside large-bore superconducting magnets (up to 15 T), enabling the low temperature and high magnetic field conditions necessary to access superconductive phase transitions or to detect single spin flip processes.

STM Imaging

STM images are generated by recording the tunneling current as a function of the tip position

while the tip is scanned across the sample surface. This can be done in two different ways which define the two main STM imaging modes:

- *Constant height mode.* The z section of the piezo scanner is kept fixed while the tip is moved over the substrate at a constant bias voltage (Fig. 3a). Variations of the tip-sample distance due to the surface topography produce a corresponding variation of the tunneling current which is recorded point-by-point and used to build the STM gray-level image. This mode is employed only in small areas of extremely flat surfaces, where the probability of crashing into protrusions such as steps or defects is relatively

small. Very high scanning speeds can be used because of the absence of a feedback control.

- *Constant current mode.* While the x and y sections of the piezo scanner are used to laterally move the tip across the surface, the z section is driven by the electronic feedback so as to maintain a constant tunneling current (Fig. 3b). The corresponding z -voltage applied to the scanner (feedback signal) is recorded point-by-point and used to build the STM gray-level image. This mode can be employed for any type of surface topography and is therefore the most frequently used.

Since the constant height mode is applied to atomically flat surfaces with sub-Å height variations, the exponential I - s relation derived from Eq. 12 can be approximated by a linear dependence. As a consequence, constant height STM images are a good representation of flat surfaces. On the other hand, for less planar substrates, one must use the constant current mode which directly reproduces the surface height due to the linear voltage-extension relation of piezoelectric materials. However, even constant current STM images are a reliable representation of the “true” surface topography only if the sample local DOS does not vary across the scanned area. If this is not the case, a constant current profile corresponds to a complex convolution of topographical and electronic features (see Eq. 12) which can be particularly relevant for surfaces covered with molecular adsorbates.

Scanning Tunneling Spectroscopy

Besides complicating the interpretation of STM images, the dependence of the tunneling current on the sample DOS also offers the unique opportunity of probing the electronic characteristics of surfaces with sub-nm spacial resolution. Having fixed the tip lateral position, the tunneling current I is a function of the applied bias voltage V and the tip-sample separation s only, the precise relation being established by Eq. 12. In a STS experiment, the relation between two of these three parameters is measured while the remaining one is kept

constant (STS). $I(V)$ spectroscopy, where the tunneling current is measured as a function of the bias voltage for a constant tip-sample separation, is the most widely used technique because it provides indications about the DOS of the sample.

Due to the spatial localization of the tunneling current (see section “Theory of Tunneling”), STS enables the characterization of the electronic properties of individual atoms and molecules in relation to their structure, bonding and local environment. Moreover, STS can also be used to create 2D maps of the sample DOS with sub-nm resolution. Such measurements are particularly interesting for quantum confined electronic systems (e.g., quantum dots or quantum corrals) or for determining the shape of molecular orbitals [14] (*wavefunction mapping*). By changing the polarity of the bias voltage, STS gives access to both the occupied and the unoccupied states of the sample. In this sense, it is often considered as complementary to ultraviolet photoemission spectroscopy (UPS), inverse photoemission spectroscopy (IPS) and electron energy loss spectroscopy (EELS), where the signal is averaged over a large area of the surface (between 0.1 and 2 mm in diameter). On the other hand, STS does not provide direct chemical information and tip artifacts can strongly influence the spectroscopic data.

So far we have assumed that electrons conserve their energy during the tunneling process (see Eq. 3). However, electrons can also tunnel inelastically between the tip and the sample by exchanging energy and inducing the excitation of vibrational modes, spin-flips, magnons, plasmons, excitons, etc. These extra tunneling channels become available only above specific voltage thresholds since only beyond these values a part of the electron energy can be converted into the excitation. The additional inelastic pathways increase the overall tunneling probability and therefore show up as discrete step-like features in the tunneling conductivity or as slope changes in $I(V)$ curves. This technique is called inelastic electron tunneling spectroscopy (IETS) and benefits from the same spatial resolution as STM and STS. IETS has been used to measure vibrational modes of individual molecules, spin excitations of single magnetic atoms, collective

plasmon excitations in 2D materials and magnons in ferromagnets.

A different way of detecting tunneling-induced molecular vibrations by means of a STM is to rely on their coupling with dynamical processes such as molecular motions. In particular, by measuring the frequency of molecular hopping events as a function of the applied bias voltage, it is possible to create so-called *action spectra* which reflect the vibrational spectrum of an individual molecule in a quantitative manner [15]. Optical excitations can also be revealed in an alternative way by coupling the STM with a photon detection system able to collect and analyze the luminescence stimulated by inelastically tunneling electrons [16]. Such a setup has been used to characterize plasmon emission from metallic surfaces and luminescence from semiconductor quantum structures and adsorbed molecules.

Applications

Since the first STM images of the surfaces of CaIrSn_4 and Au [1] were published back in 1982, STM has been used to analyze a wide range of materials: clean and adsorbate covered metal surfaces, semiconductors, superconductors, thin insulating layers, small and large organic molecules, individual atoms, liquid–solid interfaces, magnetic layers and surfaces, quasicrystals, polymers, biomolecules, nanoclusters, and carbon nanotubes. Imaging is the most frequent application of STM used to determine the structural properties of substrates and their reconstructions, the presence of defects, sites of adsorption for adatoms and molecules and the symmetry and periodicity of adsorbate superstructures. Nevertheless, right from the beginning, it became clear that the ultimate spatial resolution of STM, in combination with its dependence on the electronic properties of tip and sample, could allow a much wider range of applications of this instrument. These include the characterization of surface electronic, vibrational, optical, and magnetic properties, the measurement of single molecule conductivities, and the study of dynamic processes. In the following, we will only touch

upon some of the most frequent applications, without any presumption of being exhaustive.

Equation 12 shows that the tunneling current depends on the sample DOS close to the Fermi energy E_F . As a consequence, at a typical bias of a few Volts, it should be possible to image conductors, superconductors and small-gap or doped semiconductors but not molecules and insulating materials due to the vanishing DOS in the probed energy range (for most molecules the highest occupied and the lowest unoccupied orbitals are separated by an energy gap of several eV). However, the great majority of molecules adsorbed on metallic substrates can be easily imaged at moderate bias voltages. This is due to the formation of a metal–organic interface which can modify the molecular electronic properties leading to a broadening of the initial discrete energy levels, to a reduction of the gas-phase energy gap and even to the development of new states if covalent molecule–substrate bonds are established. All these effects contribute to the DOS at E_F and allow the imaging process. Regarding insulating materials, STM can only be done on films deposited onto conductive substrates if they are thin enough to allow the tunneling of electrons. These films are often used to electronically decouple organic adsorbates from metallic substrates.

The mechanism which allows the imaging of biomolecules such as DNA and proteins is currently still under debate [17]. As these molecules have a very large energy gap (5–7 eV) they can be considered as insulating materials and the current measured in STM experiments might be mediated by the thin water layer surrounding the molecules in air. Metalloproteins have also been imaged in their “natural” environment by using EC-STM (► EC-STM). Several reports have shown that when these redox active molecules are imaged under potentiostatic control, the tunneling current can be mediated by their metal redox-center, with enhanced conductivities measured for bias voltages close to the redox potential.

Although STM is a surface sensitive method, it can be also used to analyze buried interfaces and structures in cross-sectional STM (XSTM) [18]. The specific sample preparation in this technique requires brittle materials such as oxide samples or

semiconductor wafers. A cross section of the structure to be analyzed is prepared by cleaving the sample and positioning the STM tip onto the exposed edge. In this way, various physical properties can be probed, including the morphology and abruptness of buried nanostructures and interfaces, the alloying in epitaxial layers, the spatial distribution of dopants and their electronic configuration and the band offsets in semiconductor heterojunctions. XSTM has also been used to study, in real time, the changes occurring in semiconductor quantum well laser devices under operating conditions.

STM can further be employed for tracking dynamic surface processes, provided that the corresponding characteristic times are longer than the acquisition time. By choosing optimized designs for the piezo scanners and the electronic feedback, video-rate instruments have been developed able to record several tens of images per second and thereby to follow mobility and assembly processes in real time [19, 20].

When a tip with spin polarized electrons is used in STM, besides the parameters already indicated in Eq. 12, the local sample magnetization also influences the tunneling current. In fact, due to the different density of states at E_F of “spin-up” and “spin-down” electrons in magnetic materials, a spin polarized tip causes a tunnel magnetoresistance effect which results in a further contrast mechanism. This technique, called spin-polarized STM (SP-STM), has been used both in the presence and absence of an external magnetic field for detecting magnetic domain structures and boundaries in ferro- and antiferromagnetic materials, visualizing atomic-scale spin structures and determining spatially resolved spin-dependent DOS. An essential aspect of SP-STM is the ability to control the magnetization direction of the tip which can be achieved by evaporating different types of ferromagnetic or antiferromagnetic thin films on nonmagnetic tips. This technique is preferred to the use of bulk magnetic tips since it reduces the magnetic stray fields which can significantly modify the sample magnetization [21].

The ability of STM to identify and address individual nano-objects has been used to measure

the conductivity of single molecules absorbed on metal surfaces. While the tip is approached to the molecule of interest at constant bias voltage, the current flowing in the junction can be measured, thereby generating an $I(s)$ curve. Alternatively, $I(V)$ curves can be recorded at different s values. Since tip and substrate act as electrodes, both methods enable information to be obtained about the conductance of the individual molecule embedded in the junction. These measurements are often complemented by IETS experiments in the same configuration. IETS might in fact help to determine the arrangement and the coupling of the junction, which has a significant influence on the electronic and structural properties of the molecule. Single molecule STM conductance experiments represent an important source of information for understanding mechanisms of electron transport in organic molecules with applications in organic electronics and photovoltaics. They complement narrow gap electrode and break junction techniques, having the significant advantage of a highly localized electrode which allows to address and characterize individual molecules.

A similar type of application, although typically not aimed at individual molecules, is at the basis of the four point probe STM, where four STM tips, in addition to imaging, are used for local four point electric conduction measurements. A scanning electron microscope is installed above the STM enabling the positioning of the tips on the contact. The purpose of such very complex instruments is to measure the charge transport through individual nanoelectronic components (in particular self-assembled ones) and to correlate this information with a local high-resolution structural characterization.

Tip-Induced Modification

Besides being an extraordinary instrument for the characterization of structural, electronic, vibrational, optical, and magnetic properties of surfaces with subnanometer resolution, STM has also developed as a tool to modify and nanoengineer matter at the single molecule and atom scale.

By decreasing the distance between the tip and the sample in a controlled way, indentations can

be produced in the substrate with lateral sizes down to a few nm. Nanolithography can also be performed by tunneling electrons into a layer of e-beam photoresist (► [SU-8 Photoresist](#)), thereby reaching a better resolution compared to standard electron beam lithography (EBL). Many other STM-based nanopatterning and nanofabrication techniques have been developed based on a number of physical and chemical principles including anodic oxidation, field evaporation, selective chemical vapor deposition, selective molecular desorption, electron-beam induced effects, and mechanical contact. All these methods exploit the extreme lateral localization of the tunneling current and can be applied in air, liquids and vacuum.

However, the nanotechnological application that gained most attention is the ability to manipulate individual atoms and molecules on a substrate. This is possible due to a controlled use of tip-particle forces and is typically done in UHV and at low temperatures. The first atomic manipulation experiment was performed by Eigler and Schweizer in 1989 [2]. This phenomenal result fulfilled Richard Feynman's prophecy that "ultimately-in the great future-we can arrange the atoms the way we want; the very atoms, all the way down!" [3].

During a lateral manipulation experiment, the tip is first placed above the particle to be moved (for example an atom) and the tunneling current is increased while keeping a constant voltage. This results in a movement of the tip toward the atom, see Eq. 12. If their separation is reduced below 0.5 nm, Van der Waals forces start to come into play together with attractive and repulsive chemical interactions. When these forces equal the diffusion energy barrier, a lateral displacement of the tip can induce a movement of the atom parallel to the surface. After the desired final position is reached, the tip is retracted by reducing the tunneling current to the initial value, leaving the atom in the selected place. Depending on the tip-particle distance and therefore on the strength and nature of the interaction, different manipulation modes including pulling, pushing, and sliding [22] were identified and used to move different types of atoms and molecules.

Thanks to this technique, it was possible to fabricate artificial nanostructures such as the *quantum corral* [23] and to probe quantum mechanical effects like the quantum confinement of surface state electrons or the *quantum mirage*. Lateral STM manipulation has also been used to switch between different adsorption configurations and conformations of molecules on surfaces and to modify their electronic properties in a controlled way [24].

A further application of STM manipulation is the synthesis of new molecular species based on the ability of STM to form and break chemical bonds with atomic precision. Reactants are brought close together on the surface and the actual reaction is realized by applying a voltage pulse or by exciting vibrational modes through inelastically tunneling electrons. Examples of this technique include the dissociation of diatomic molecules, the Ullmann reaction, the isomerization of dichlorobenzene and the creation of metal-ligand complexes.

The STM tip has also been used to perform vertical manipulations of nanoparticles where an atom (or molecule) is deliberately transferred from the surface to the tip and vice versa by using the electric field generated by the bias voltage. In contrast to the lateral manipulation, here the bonds between the surface and the atom are broken and re-created [25]. By approaching the tip at distances of a few Å from the chosen particle chemical interactions are established that reduce the atom-surface binding energy. If a voltage pulse is applied under these conditions, the resulting electric field (of the order of 10^8 V/cm) can be enough to induce the particle desorption. The vertical manipulation technique has also been used as a means to increase the lateral resolution of STM. In fact, the controlled adsorption of a specific molecule onto the tip often makes it "sharper" and can add a chemical resolution capability if the DOS of the extra molecule acts as an "energy filter."

A related effect is exploited in the recently proposed scanning tunneling hydrogen microscopy (STHM) technique. In STHM, the experimental chamber is flooded with molecular hydrogen while the tip is scanned in constant

height mode at very close distances over the surface. H_2 can get trapped in the tip-sample junction and its rearrangement during scanning of the surface generates a new contrast mechanism based on the short-range Pauli repulsion. This is extremely sensitive to the total electron density, thereby endowing the STM with similar imaging capabilities to non-contact AFM (► [AFM, Noncontact Mode](#)) and making it able to resolve the inner structure of complex organic molecules [26].

Acknowledgments This work was supported by EPSRC (EP/D000165/1); A. Della Pia was funded through a WPRS scholarship of the University of Warwick. J. V. Macpherson, T. White, and B. Moreton are gratefully thanked for their critical reading of the manuscript.

Cross-References

- [AFM, Noncontact Mode](#)
- [Atomic Force Microscopy](#)
- [Electrochemical Scanning Tunneling Microscopy](#)
- [Electron Beam Lithography \(EBL\)](#)
- [Piezoresistivity](#)
- [Scanning Electron Microscopy](#)
- [SU-8 Photoresist](#)
- [Transmission Electron Microscopy](#)

References

1. Binnig, G., Rohrer, H., Gerber, C., Weibel, E.: Surface studies by scanning tunneling microscopy. *Phys. Rev. Lett.* **49**, 57 (1982)
2. Eigler, D.M., Schweizer, E.K.: Positioning single atoms with a scanning tunneling microscope. *Nature* **344**, 524 (1990)
3. Feynman, R.P.: There's plenty of room at the bottom: an invitation to enter a new field of physics. *Eng. Sci.* **23**, 22 (1960)
4. Bardeen, J.: Tunneling from a many-particle point of view. *Phys. Rev. Lett.* **6**, 57 (1961)
5. Gottlieb, A.D., Wesoloski, L.: Bardeen's tunnelling theory as applied to scanning tunnelling microscopy: a technical guide to the traditional interpretation. *Nanotechnology* **17**, R57 (2006)
6. Lang, N.D.: Spectroscopy of single atoms in the scanning tunneling microscope. *Phys. Rev. B* **34**, 5947 (1986)
7. Landau, L.D., Lifshitz, E.M.: *Quantum Mechanics: Non-relativistic Theory*. Pergamon Press, Oxford (1977)
8. Chen, C.J.: *Introduction to Scanning Tunneling Microscopy*. Oxford University Press, Oxford (2008)
9. Binnig, G., Rohrer, H.: Scanning tunneling microscope. *Helv. Phys. Acta* **55**, 726 (1982)
10. Okumura, A., Miyamura, K., Gohshi, Y.: The STM system constructed for analytical application. *J. Microsc.* **152**, 631 (1988)
11. Besocke, K.: An easily operable scanning tunneling microscope. *Surf. Sci.* **181**, 145 (1987)
12. Pan, S.H., Hudson, E.W., Davis, J.C.: ^3He refrigerator based very low temperature scanning tunneling microscope. *Rev. Sci. Instrum.* **70**, 1459 (1999)
13. Laegsgaard, E., et al.: A high-pressure scanning tunneling microscope. *Rev. Sci. Instrum.* **72**, 3537 (2001)
14. Repp, J., Meyer, G., Stojkovic, S.M., Gourdon, A., Joachim, C.: Molecules on insulating films: scanning-tunneling microscopy imaging of individual molecular orbitals. *Phys. Rev. Lett.* **94**, 026803 (2005)
15. Sainoo, Y., et al.: Excitation of molecular vibrational modes with inelastic scanning tunneling microscopy processes: examination through action spectra of cis-2-butene on Pd(110). *Phys. Rev. Lett.* **95**, 246102 (2005)
16. Gimzewski, J.K., Reihl, B., Coombs, J.H., Schlittler, R.R.: Photon emission with the scanning tunneling microscope. *Z. Phys. B: Condens. Matter* **72**, 497 (1988)
17. Davis, J.J.: Molecular bioelectronics. *Philos. Trans. R. Soc. A* **361**, 2807 (2003)
18. Feenstra, R.M.: Cross-sectional scanning-tunneling-microscopy of III-V semiconductor structures. *Semicond. Sci. Technol.* **9**, 2157 (1994)
19. Rost, M.J., et al.: Scanning probe microscopes go video rate and beyond. *Rev. Sci. Instrum.* **76**, 053710 (2005)
20. Petersen, L., et al.: A fast-scanning, low- and variable-temperature scanning tunneling microscope. *Rev. Sci. Instrum.* **72**, 1438 (2001)
21. Wiesendanger, R.: Spin mapping at the nanoscale and atomic scale. *Rev. Mod. Phys.* **81**, 1495 (2009)
22. Bartels, L., et al.: Dynamics of electron-induced manipulation of individual CO molecules on Cu (111). *Phys. Rev. Lett.* **80**, 2004 (1998)
23. Crommie, M.F., Lutz, C.P., Eigler, D.M.: Confinement of electrons to quantum corrals on a metal-surface. *Science* **262**, 218 (1993)
24. Moresco, F., et al.: Conformational changes of single molecules induced by scanning tunneling microscopy manipulation: a route to molecular switching. *Phys. Rev. Lett.* **86**, 672 (2001)
25. Avouris, P.: Manipulation of matter at the atomic and molecular-levels. *Acc. Chem. Res.* **28**, 95 (1995)
26. Weiss, C., et al.: Imaging Pauli repulsion in scanning tunneling microscopy. *Phys. Rev. Lett.* **105**, 086103 (2010)

Scanning Tunneling Spectroscopy

Amadeo L. Vázquez de Parga and
Rodolfo Miranda

Department of Física de la Materia Condensada,
Universidad Autónoma de Madrid and Instituto
Madrileño de Estudios Avanzados en
Nanociencia (IMDEA-Nanociencia), Madrid,
Spain

Definition

Scanning tunneling spectroscopy (STS) is a technique that allows the study of the electronic structure of surfaces with atomic resolution.

Overview

Scanning tunneling microscopy (STM) was historically the second technique that could image individual atoms one by one. It was invented in 1981–1982 by Gerd Binnig and Heinrich Rohrer [1], long after the technique of field ion microscopy (FIM) developed in 1951 by Erwin Müller [2].

In STM a sharp tip probes the surface of interest by allowing electrons to tunnel quantum mechanically between the tip and the surface. Because such tunneling is extremely sensitive to the distance between tip and surface, one gets high resolution perpendicular to the surface. Assuming a constant density of states on the surface, when the STM tip is scanned over the sample surface while keeping the tunneling current constant, the tip movement depicts the surface topography, because the separation between the tip apex and the sample surface is always constant. It is worth noting that STM not only converts the spatial change in the tunneling current into a highly detailed topographic image of surfaces with constant density of states but also the tunneling current changes with the available surface electronic states. This dependence of the tunneling current on the surface electronic structure together with

the high spatial resolution of STM allows us to study the electronic structure of the surfaces with atomic resolution. The technique is known as scanning tunneling spectroscopy (STS).

Scanning Tunneling Spectroscopy Theory

Most theoretical treatments applied today to describe the tunneling process in an STM start from the formalism of the transfer Hamiltonian developed by Bardeen in 1961 [3] for the study of superconducting tunnel junctions. In this approach, the electronic structure and electron wave functions of both electrodes are calculated assuming no interaction between them and afterward the tunneling current is calculated [3]. Figure 1a shows the scheme of the tunnel junction in an STM where one of the electrodes is a tip. Figure 1b shows the energy diagram of the tunnel junction. In this diagram, the vertical axis represents energy. E_t and Ψ_t are the energy and wave function of the states of the electrode “tip” in the absence of electrode “sample.” E_s and Ψ_s are the energy and wave function of the states of the electrode “sample” in the absence of electrode “tip.” ϕ_t , ϕ_s , E_F^t , E_F^s , ρ_t , and ρ_s are the work functions, Fermi energies, and densities of states (DOS) of electrode “tip” and “sample,” respectively, and V is the voltage applied to electrode “sample.” When the distance between the electrodes is small enough, the overlap between their wave functions is significant, and the probability of electron transfer between the two electrodes by tunneling starts to be noticeable. In the absence of applied voltage, the Fermi levels of the two electrodes are aligned and no net tunneling current flows. However, by applying a voltage V , the Fermi levels move with respect to each other opening an energy window, eV , where electrons from one electrode can tunnel to the empty states of the other and, thus, the tunneling current starts to flow.

In 1983, Tersoff and Hamann applied the Bardeen’s formalism to the STM, replacing one of the electrodes by a point [4–6]. The tip was